Journal of Advanced Marine Engineering and Technology, Vol. 46, No. 2, pp. 56~63, 2022
J. Advanced Marine Engineering and Technology (JAMET)
https://doi.org/10.5916/jamet.2022.46.2.56

ISSN 2234-7925 (Print)
ISSN 2765-4796 (Online)
Original Paper

Experimental investigation of ringing intensity and combustion noise level from biodiesel fuel in CRDI diesel engine with various injection timings

Hyun Min Baek[1] · Hyung Min Lee†

(Received February 24, 2022 ; Revised March 17, 2022 ; Accepted March 17, 2022)

Graphical Abstract

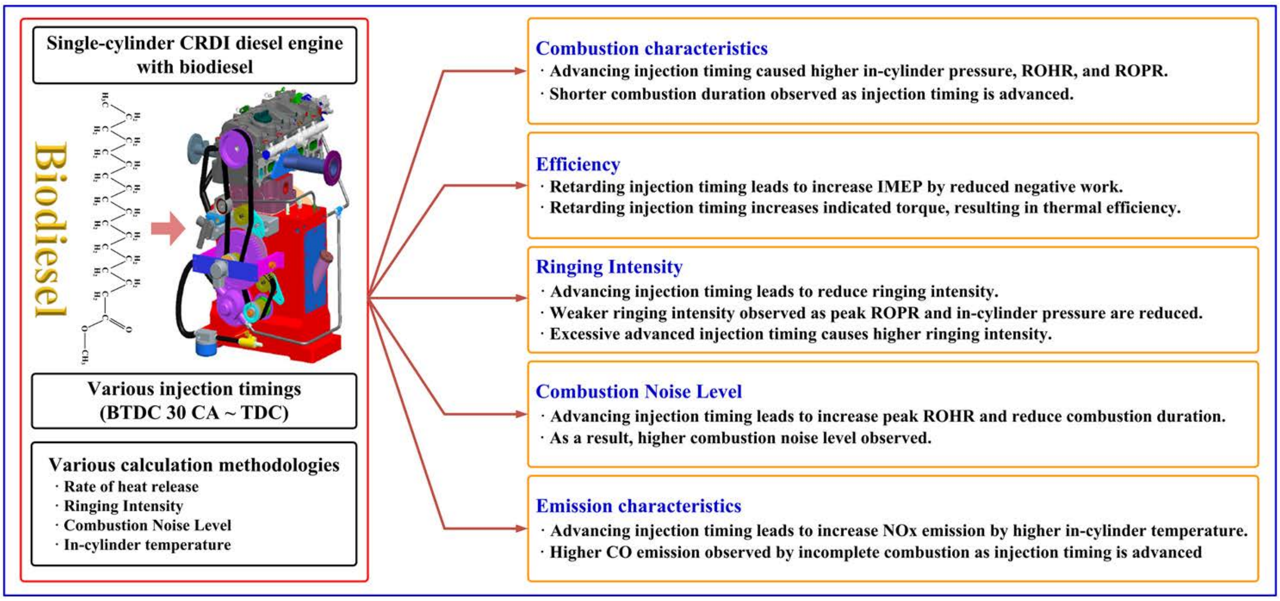

Abstract: In this study, the effect of fuel-injection timing on ringing intensity and combustion noise level in a single-cylinder common-rail direct-injection diesel engine (CRDI) operating on biodiesel fuel is quantitatively investigated. Various combustion characteristics such as in-cylinder pressure, rate of heat release (ROHR), rate of pressure rise (ROPR), and in-cylinder temperature are analyzed. In addition, emissions such as carbon monoxide (CO) and nitrogen oxides (NOx) are analyzed based on different fuel-injection timings. It is observed that the peak in-cylinder pressure, ROHR, ROPR, and in-cylinder temperature levels increase as the fuel-injection timing is advanced. Advancing the injection timing deteriorates the engine performance, as indicated by the mean effective pressure, torque, and thermal efficiency. It is discovered that a more intense premixed combustion resulting from longer ignition delays during advanced fuel-injection timings results in increased ringing intensity (RI) and combustion noise levels (CNL). As the fuel-injection timing is advanced, the CO and NOx emission levels increase because of incomplete combustion and higher in-cylinder temperatures.

Keywords: Ringing intensity, Combustion noise level, Combustion characteristics, Emission, Engine performance

Abbreviations

ABDC	After before dead center
ATDC	After top dead center
BBDC	Before top dead center
BTDC	Before top dead center
CA	Crank angle
CA50	10% MFB to 50% MFB
CNL	Combustion noise level
CO	Carbon monoxide
CRDI	Common rail direct injection

† Corresponding Author (ORCID: http://orcid.org/0000-0003-1999-2604): Professor, Department of Navigation and Ship Handling System, Republic of Korea Naval Academy, (51704) Box 88-1, Jinhaegu, Changwonsi, Kyungsangnmdo, Korea, E-mail: hmsj1226@korea.ac.kr, Tel: 055-907-5345

1 Assistant professor, Department of Navigation and Ship Handling System, Republic of Korea Naval Academy, E-mail: jeapo2812@naver.com, Tel: 055-907-5346

EGR	Exhaust gas recirculation
GMT	Gas mean temperature
IMEP	Indicated mean effective pressure
MFB	Mass fraction burned
P_{peak}	Peak in-cylinder pressure
RI	Ringing intensity
ROHR	Rate of heat release
ROPR	Rate of pressure rise
TDC	Top dead center
m_f	Fuel mass
Q_{LEV}	Lower heating value

1. Introduction

Electronic fuel injectors in diesel engines enable the diversification of fuel-injection methods, such as those pertaining to precise fuel-injection quantities, fuel-injection timings, and fuel-injection-frequency controls. Among these diversification methods, fuel-injection timing is one of the key variables affecting engine performance, including engine noise, vibration, and emission levels. Several studies have indicated that combustion characteristics such as the in-cylinder pressure, peak rate of heat release (ROHR), and peak rate of pressure rise (ROPR) increase as the fuel-injection timing shifts from the top-dead-center (TDC) to advanced **[1]-[3]**. Advanced injection timing causes a long ignition delay and hence improves the air–fuel mixture. However, fuel injection at low cylinder pressures and temperatures causes significant wall wetting, which results in increased carbon monoxide (CO) emissions **[4]-[6]**. In addition, combustion as a result of early injection increases the intensity of the premixed combustion and causes the gas temperature and level of nitrogen oxides (NOx) to increase, which results in deteriorated engine performance **[7]-[8]**. Fuel-injection timing can be improved using a tool that can reduce engine/combustion noise and vibration while utilizing the same amount of fuel. Researchers have introduced ringing intensity (RI) as a quantitative indicator to evaluate engine noise and vibration. It has been reported that high levels of ROHR and ROPR with high premixed combustion during the initial combustion result in high RIs. Meanwhile, the combustion noise level (CNL) is closely associated with the fuel-injection timing and overall combustion duration. It has been reported that as the fuel-injection timing advances, the CA50 (10% MFB to 50% MFB; MFB = mass fraction burned), defined as the rapid combustion period, decreases, and the overall combustion duration (10% MFB to 90% MFB) is reduced. Consequently, the combustion noise level is increased.

Biodiesel is an eco-friendly fuel that contains oxygen and can be mixed with diesel fuel in an appropriate ratio without requiring engine modifications. In fact, biodiesel can reduce ignition delays and reduce the RI. **Table 1** summarizes the findings obtained from previous studies pertaining to RIs and CNLs **[9]-[15]**. The current study was conducted to quantitatively analyze the RI and CNL based on the fuel-injection timing using various combustion parameters by applying biodiesel to an experimental single-cylinder common-rail direct-injection diesel engine. The results of this study revealed that advancing the injection timing adversely affected the RI and CNL.

Table 1: Review of studies pertaining to RI and CNL

[#] Authors	Main contents
[9] S. Erdogan *et al*.	· Ringing intensity was lower with the use of biodiesel.
[10] S. Polat *et al*.	· The ringing intensity increased when injection timing was advanced. · The rate of pressure rise and the tendency of knocking increased at excess low-air coefficient values.
[11] M. H Choi *et al*.	· The combustion of a single injection had a long ignition delay, which led to premixed combustion. · As a result of the high intensity of premixed combustion, severe engine noise and vibration occurred. · The main objective of the pilot injection was to prevent engine noise and vibration.
[12] G. Shibata *et al*.	· The initial rise in the high-temperature heat release was related to the engine noise. · Thermal efficiency increased when the connecting rod/crank-radius ratio decreased.
[13] J. Dernotte *et al*.	· The ringing intensity correlated to the propensity of the combustion process to produce an acoustically resonating wave-leading knock, and it may be a better criterion for combustion testing aimed at reducing unwanted knocking during combustion. · In contrast, the combustion noise level was a valuable indicator of the overall loudness of the combustion, regardless of whether or not a strong acoustic resonance was present.
[14] R. K. Maurya *et al*.	· The ringing intensity increased with an equivalence ratio of constant inlet temperature at all engine speeds. · The sensitivity of the ringing intensity with equivalence ratio increased when the engine speeds increased.
[15] S. Braekaert *et al*.	· During ringing combustion, heat flux and the fraction of the energy lost peaked as the heat increased.

2. Experimental System

2.1 Experimental setup

Figure 1 shows a schematic illustration of the configuration of the test device. A single-cylinder CRDI diesel engine equipped with a sac-type injector was used to perform the test; the specifications of the test engine are summarized in **Table 2**. Various devices were constructed to perform the test. **Table 3** lists the main functions of the devices constructed, as shown in **Figure 1**. The single-cylinder CRDI diesel engine maintained a constant speed via a 22 kW electric motor. The energy generated by the engine was dissipated by a braking resistor connected to an electric motor.

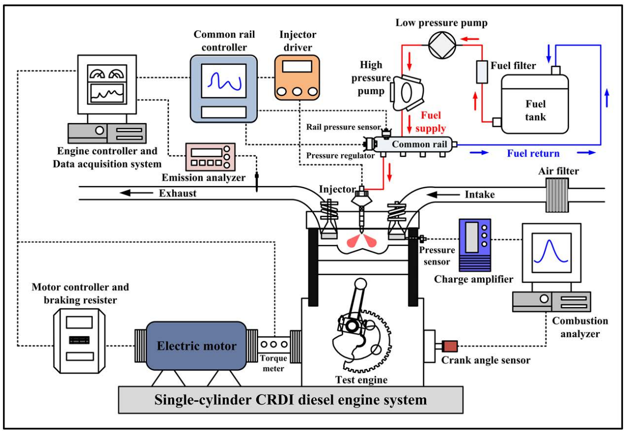

Figure 1: Schematic illustration of experimental system

Table 2: Specifications of test engine

Item	Descriptions	
Engine type	4-stroke, Single-cylinder CRDI	
Number of cylinder	1	
Bore × Stroke	83 mm × 92 mm	
Compression ratio	17.7 : 1	
Displacement	498 cc	
Valve timing	IVO	BTDC 7 CA
	IVC	BTDC 43 CA
	EVO	BBDC 52 CA
	EVC	ATDC 6 CA

2.2 Experimental conditions and test fuel

In this study, a single fuel-injection timing strategy without pilot injection was applied. The test was conducted while adjusting the fuel-injection timing from before the top dead center (BTDC) 30 crank angle (CA) to TDC at 5 CA units. The experiment was performed with the speed of the test engine fixed at 1100 rpm, a fuel injection amount of 10 mg, and a fuel-injection pressure of 40 MPa. The in-cylinder pressure was averaged by measuring 300 cycles to minimize cycle-to-cycle fluctuations. **Table 4** lists the experimental conditions for reference. The physicochemical properties of the test fuel, compared with those of the diesel fuel used in naval vessels, are listed in **Table 5**.

Table 3: Function of main devices constituting experimental system

Instruments	Main function (Model)
Test engine	Single-cylinder CRDI diesel engine (MD-SDE-100)
22 kW electric motor	Precisely control speed (HV2 induction motor)
Injection controller	Injection control (ZB-5100)
Exhaust gas analyzer	Measure CO and NOx (Testo-350K)
Piezoelectric pressure sensor	Measure the in-cylinder pressure (Type 6056A)
Amplifier	Measure the in-cylinder pressure (Type 5018)
Combustion analyzer	Analyze the combustion characteristic (MT-7000S)
Engine control system	Control parameters such as injection duration, engine speed, injection pressure

Table 4: Settings used in experiment

Parameter		Description
Engine speed		1100 rpm
P_{inj}		40 MPa
Fuel injection mass		10 mg
Coolant temperature		80°C
EGR rate		N/A
Intake temperature		Room temperature
Measuring Duration	In-cylinder	300 cycle
	Emission	

Table 5: Physiochemical properties of BD100

Properties	Values	
	BD100	Diesel
Carbon (wt %)	77.71	86.97
Hydrogen (wt %)	13.05	12.64
Density(kg/m^3,15 °C)	882.7	849.4
Kinematic viscosity (mm^2/s)	4.341	3.621
Cetane number	56.3	52.8
Lower heating value (kJ/kg)	37,910	42,710

2.2 Methodology for analysis RI and CNL

Based on the same operating conditions of the engine, adjusting the fuel injection timing can be an effective strategy for improving engine vibration and noise. To confirm this hypothesis, a method for quantifying engine vibration and noise is required. To date, the most effective method for analyzing engine vibration and noise is by using a measurement device **[16]-[18]**. However, in this study, the RI and CNL were quantified by applying a theoretical methodology that has been verified by researchers, without using a direct measuring device. The RI representing knocking combustion can be expressed as follows **[19]**:

$$RI = \frac{\sqrt{\gamma R T_{peak}}}{2\gamma P_{peak}}\left[\beta\left(\frac{dP}{dt}\right)_{peak}\right] \quad (1)$$

Where γ represents the ratio of specific heat, $\left(\frac{dP}{dt}\right)_{peak}$ the peak ROPR, P_{peak} the peak in-cylinder pressure, T_{peak} the peak in-cylinder temperature, R the ideal gas constant, and β = 0.05 ms a constant value. The RI was simulated by calculating the ROPR and in-cylinder temperature using the measured in-cylinder pressure. The ROHR (**Equation (2)**) was calculated based on the first law of thermodynamics and **Equation (3)**. Meanwhile, **Equation (4)** was applied to the in-cylinder temperature **[20][21]**.

$$\frac{dQ}{d\theta} = \frac{\gamma}{\gamma-1}P\frac{dV}{d\theta} + \frac{1}{\gamma-1}V\frac{dP}{d\theta} \quad (2)$$

$$T(\theta) = \frac{P(\theta)V(\theta)}{m_{intake}R}, \quad m_{intake} = v_l \rho_{air} V_{IVC} \quad (3)$$

$$v_l = \frac{1}{2}\left\{\sin\left[360\left(\frac{\theta}{\theta_{vod,intake}} - \frac{1}{\theta_{vod,\frac{intake}{exhaust}}}\theta_{\frac{IVO}{EVO}} - \frac{1}{4}\right)\right] + 1\right\} \quad (4)$$

In **Equation (2)**, P is the measured in-cylinder pressure, V the cylinder volume to corresponding to the CA of the test engine, and γ the specific heat ratio. In **Equations (3)** and **(4)**, P, V, and T represent the in-cylinder pressure, volume, and in-cylinder temperature, respectively; m_{intake} is the intake air mass at intake-valve closing; ρ_{air} is the air density; V_{ivc} is the cylinder volume at intake-valve closing; v_l is the function of valve lift; $\Theta_{vod,intake}$ is the intake-valve opening duration; $\Theta_{vod,exhaust}$ is the exhaust-valve opening duration; Θ_{IVO} and Θ_{EVO} are the intake-valve opening and exhaust-valve opening angles, respectively. Because the ROPR was applied as a time ratio in the RI equation, the ROPR that had been calculated using the CA ratio was changed to the time ratio to quantify the RI. To quantify the CNL characteristics, the statistical analysis proposed previously and the equation that established the experimental correlation between the variables of the peak ROHR and combustion period were applied in this study. The equation to quantify the CNL can be expressed as follows **[16][21]**:

$$CNL = -0.544(\mathrm{CD}) + 0.0275(ROHR)_{peak} + 85.526 \quad (5)$$

Where CD represents the combustion duration between 10% and 90% MFB, and $ROHR_{peak}$ is the peak rate of the pressure rise.

3. Results and Discussions

3.1 Combustion characteristics

Figure 2 shows the effects of the fuel-injection timing on the in-cylinder pressure, ROHR, and ROPR.

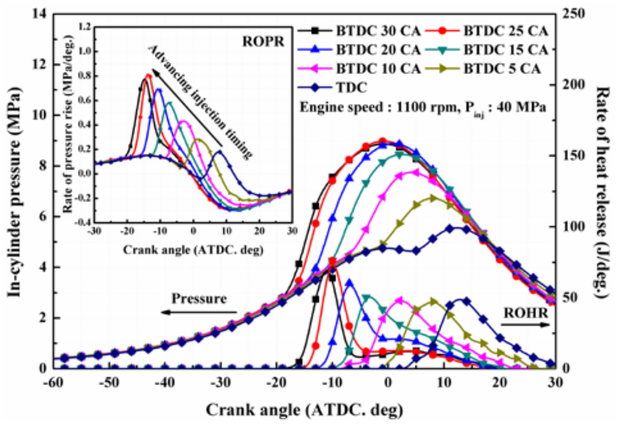

Figure 2: In-cylinder pressure, ROHR, and ROPR characteristics with various injection timings corresponding to crank angle

As the fuel-injection timing advanced, the peak in-cylinder pressure, ROHR, and ROPR values increased. When the fuel injection was advanced and the in-cylinder pressure and temperature were low, the mixture formation improved significantly owing to a longer ignition delay, thereby resulting in a higher premixed combustion intensity, and hence higher peak ROHR and ROPR values. In addition, because the advanced combustion directly affected the compression stroke, it exerted an adverse effect. A higher mixture-formation intensity and ignition delay reduced the overall combustion period, which consequently decreased the indicated mean effective pressure (IMEP).

The effect of the fuel-injection timing on the engine performance was confirmed. **Figure 3** shows a comparison of the results of the IMEP, indicated torque, and thermal efficiency based on the fuel-injection timing. The formulas for calculating the IMEP, indicated torque, and thermal efficiency are as follows:

$$IMEP = \frac{\Delta\theta}{V_d}\sum_{i=n_1}^{n_2} P(i)\frac{dV(i)}{d\theta} \quad (6)$$

$$Indicated\ torque = \frac{imep\ V_d}{4\pi} \quad (7)$$

$$Indicated\ thermal\ efficiency = \frac{Indicated\ work}{Q_{in}(m_f Q_{LEV})} \quad (8)$$

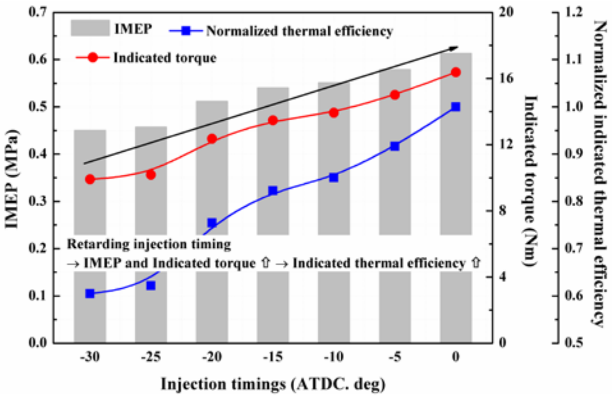

Figure 3: IMEP, Indicated torque, and Normalized indicated thermal efficiency characteristics with various injection timings

In **Equations (6), (7),** and **(8)**, V_d represents the swept volume, m_f the injection fuel mass, and Q_{LEV} the lower heating value of the biodiesel. As shown in **Figure 3**, the IMEP, indicated torque, and thermal efficiency increased as the fuel-injection timing approached the TDC. The in-cylinder pressure and temperature were high under retarded conditions. This reduced the ignition delay period, resulting in an improved combustion efficiency. As the fuel-injection timing was delayed, the adverse effects diminished, whereas the positive effects became more prominent; hence, the engine performance improved. In addition, retarding the fuel-injection timing while maintaining a constant heat release (m_fQ_{LEV}) improved the fuel conversion efficiency and combustion efficiency, which consequently improved the thermal efficiency.

3.2 RI and CNL characteristics

To calculate the RI, combustion parameters, such as the peak ROPR, peak in-cylinder pressure, and peak in-cylinder pressure were considered. According to various studies, an acceptable RI value is 5 MW/m^2 **[19][22]**. **Figure 4** presents the results of RI, peak ROPR, and peak in-cylinder pressure vs. fuel-injection timing. As mentioned above, the advanced fuel-injection timing increased the intensity of the premixed combustion, which consequently increased the peak in-cylinder pressure and ROPR. In addition, the peak in-cylinder temperature increased, as per **Equations (3)** and **(4)**. RI is an index used to quantitatively evaluate the strength of knocking by combustion and is associated closely with engine noise and vibration. The highest RI was indicated at BTDC 25 CA; in fact, the RI decreased as the fuel-injection timing was retarded toward the TDC. The RI decreased because the retarded fuel injection suppressed the premixed combustion and improved the combustion stability. In particular, it was evaluated to be below the RI limit of BTDC 15 CA.

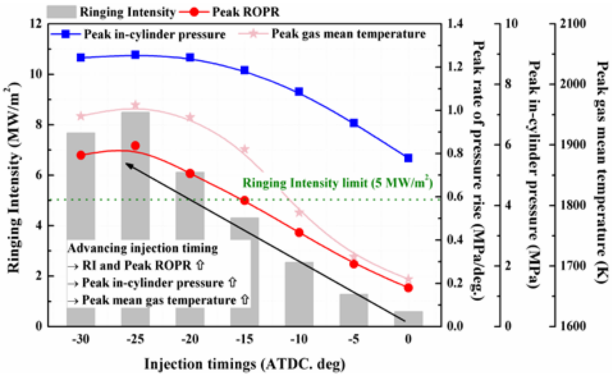

Figure 4: Ringing intensity, peak ROPR, peak in-cylinder pressure, and Peak gas mean temperature vs. injection timing

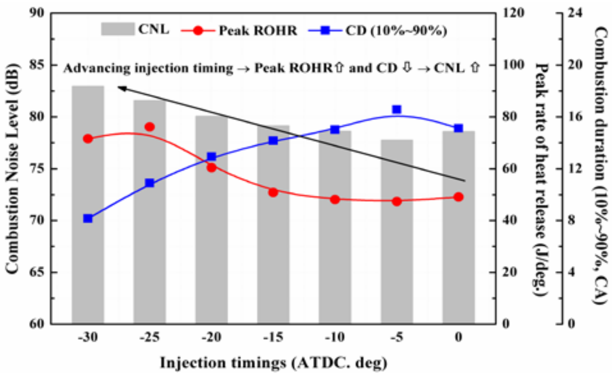

Figure 5: Combustion noise level, peak ROHR, and combustion duration characteristics vs. injection timing

Figure 5 provides the analysis results of the effects of the fuel-injection timing on the CNL, the peak ROHR, and the overall combustion duration. In this study, the variables for evaluating the CNL based on the fuel-injection timing were the peak ROHR and overall combustion duration that affected the combustion process **[16][21]**. As the fuel-injection timing advanced, the combustion duration decreased and the peak ROHR increased. Under more advanced conditions, the additional time for mixture formation and ignition delay increased the premixed combustion intensity and reduced the combustion period. A strong premixed combustion and a short combustion period resulted in a high CNL. As the fuel-injection timing was delayed, the CLN decreased gradually as the combustion phase (CA50) was generated in the expansion stroke.

3.3 Emission characteristics

Figure 6 shows the effect of fuel-injection timing on CO,

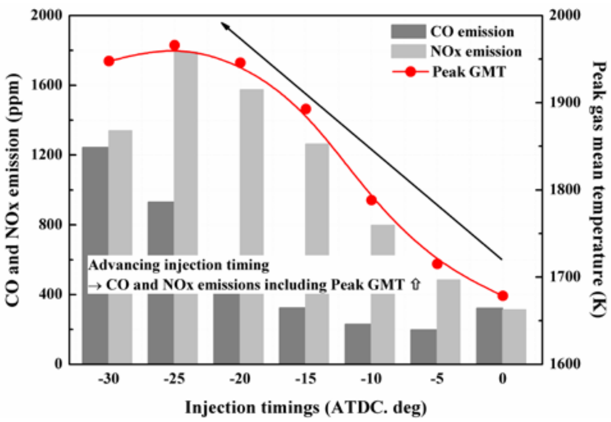

Figure 6: CO, NOx, and peak gas mean temperature vs. injection timing

NOx, and peak gas mean temperature (GMT).

Our analysis showed that CO, NOx, and the peak GMT increased as the fuel-injection timing advanced from the TDC. At the early injection point, the spray of the injected fuel developed rapidly because of the lower in-cylinder pressure and temperature. Therefore, local piston wall-wetting was generated, and incomplete combustion occurred owing to the weaker oxidation. This was considered a key contributor to the increase in CO. The NOx was considered thermal NOx, which is associated closely with the combustion gas temperature during the combustion reaction stage. Advancing the injection timing increased the intensity of the premixed combustion via the formation of a superior mixture with a longer ignition delay, as well as via an increase in the peak ROHR and combustion gas temperature. Significant NOx formation was observed as the injection timing became more advanced.

4. Conclusions

An experimental analysis was conducted to quantify the RI and CNL by applying various injection timings of biodiesel fuel in a single-cylinder CRDI diesel engine. The main conclusions of this experimental investigation are summarized as follows:

1) Advancing the injection timing resulted in increased peak in-cylinder pressure, ROHR, and ROPR levels. However, the values of engine performance indicators, such as the IMEP, indicated torque, and thermal efficiency, decreased during the compression stroke of combustion.
2) RI, as an indicator of engine noise and vibration levels, increased as the fuel-injection timing advanced from the TDC. This was due to the long ignition delays, which increased the intensity of premixed combustion. In particular, our results exceeded the limit of the RI value under premature injection conditions (BTDC 20–30 CA). Advancing the injection timing reduced the overall combustion duration and increased the peak ROHR owing to the more intense premixed combustion. Consequently, the CNL increased in response to each advance in the fuel-injection timing.
3) As the fuel-injection timing was advanced, a significant level of CO emissions was observed during incomplete combustion and weaker oxidation reactions. In addition, advancing the injection timing resulted in higher peak ROHR and in-cylinder temperatures, which consequently increased NOx emissions.

Acknowledgement

This study was supported by the 2022 Academic Research Project of the Naval Institute for Ocean Research of the Republic of Korea Naval Academy.

Author Contributions

Conceptualization, H. Lee; Methodology, H. Lee; Formal Analysis, H. Lee and H. -M. Baek; Investigation, H. -M. Baek; Resources, H. -M. Baek; Data Curation, H. -M. Baek; Writing-Original Draft Preparation, H. -M. Baek; Writing-Review & Editing, H. Lee.

References

[1] H. Lee, “Effects of multiple uniformity split injection strategies on combustion and exhaust emission characteristics in a single-cylinder diesel engine,” Journal of Advanced Marine Engineering and Technology, vol. 44, no. 2, pp. 117-125, 2020. Available: https://doi.org/10.5916/jamet.2020.44.2.117.

[2] K. M. V. Ravi Teja, P. Issac Prasad, K. V. K Reddy, N. R. Banapurmath, M. E. M Soudagar, N. Hossain, A. Afzal, and C. Ahamed Saleel, “Comparative analysis of performance, emission, and combustion characteristics of a common rail direct injection diesel engine powered with three different biodiesel blends,” Energies, vol. 14, no. 18, p. 5597, 2021. Available: https://doi.org/10.3390/en14185597.

[3] N. T. Nghia, N. X. Khoa, W. J. Cho, and O. T. Lim. “A study the effect of biodiesel blends and the injection timing on performance and emissions of common rail diesel engines,” Energies, vol. 15, no. 1, p. 242, 2022. Available: https://doi.org/10.3390/en15010242.

[4] Y. Zhang, Y. Zhong, J. Wang, D. Tan, Z. Zhang, and D. Y. Yang, “Effects of different biodiesel-diesel blend fuel on combustion and emission characteristics of a diesel engine,” Processes, vol. 9, no. 11, p. 1984, 2021. Available: https://doi.org/10/3390/pr9111984.

[5] J. L. Xue, T. E. Grift, and A. C. Hansen, “Effect of biodiesel on engine performances and emissions,” Renewable and Sustainable Energy Reviews, vol. 15, no. 2, pp. 1098-1116, 2011. Available: doi: 10.1016/j.rser.2010.11.016.

[6] Ö. Can, E. Özturk, and H. S. Yücesu, “Combustion and exhaust emissions of canola biodiesel blends in a single cylinder DI diesel engine,” Renewable Energy, vol. 109, pp. 73-82, 2017. Available: http://dx.doi.org/10.1016/j.renene.2017.03.017.

[7] M. Mourad, K. R. M Mahmoud, and E. H. NourEldeen, “Improving diesel engine performance and emissions characteristics fueled with biodiesel,” Fuel, vol. 302, p. 121097, 2021. Available: https://doi/org/10.1016/j.fuel.2021.121097.

[8] S. Polat, “An experimental investigation on combustion, performance and ringing operation characteristics of a low compression ratio early direct injection HCCI engine with ethanol fuel blends,” Fuel, vol. 277, p. 118092, 2020. Available: https://doi.org/10.1016/j.fuel.2020.118092.

[9] S. Erdogan, M. K. Balki, and C. Sayin, “The effect on the knock intensity of high viscosity biodiesel use in a DI diesel engine,” Fuel, vol. 253, pp. 1162-1167, 2019. Available: https://doi/org/10.1016/j.fuel.2019.05.114.

[10] S. Polat, H. S. Yucesu, H. Solmaz, A. Uyumaz, K. Kannan, and M. Shahbakhti, “An experimental study on the variation of COVIMEP and ringing intensity at different air excess coefficients in a HCCI engine,” International Symposium on Automotive Science and Technology, pp. 1-9, 2019. Available: https://sites.ualberta.ca/~mahdi/Docs/ISATECH_2019_HCCIExpStudy.

[11] M. H. Choi and S. W. Park, “Optimization of multiple-stage fuel injection and optical analysis of the combustion process in a heavy-duty diesel engine,” Fuel Processing Technology, vol. 228, p. 107137, 2022. Available: https://doi.org/10.1016/j.fuproc. 2021.107137.

[12] G. Shibata, K. Ishi, H. Ushijima, Y. Shibike, H. Ogawa, and D. E. Foster, Optimization of Heat Release Shape and the Connecting Rod Crank Radius Ratio for Low Engine Noise and High Thermal Efficiency of Premixed Diesel Engine Combustion, SAE Technical Paper, 2015-01-0825, SAE International, USA, 2015. Available: https://doi.org/10.4271/2015-01-0825.

[13] J. Dernotte, J. E. Dec, and C. S. Ji, Investigation of the Sources of Combustion Noise in HCCI Engines, SAE Technical Paper, 2014-01-1272, SAE International, USA, 2014. Available: https://doi.org/10.4271/2014-01-1272.

[14] R. K. Maurya and M. R. Saxena, “Characterization of ringing intensity in a hydrogen-fueled HCGI engine,” International Journal of Hydrogen Energy, vol. 43, no. 19, pp. 9423-9437, 2018. Available: https://doi.org/10.1016/j.ijhydene.2018.03.194.

[15] S. J. Broekaert, K. Chana, M. de Paepe, and S. Verhelst, “The effect of ringing combustion on the wall heat flux during HCCI operation,” FISITA automotive conference, F2019-ESYB-005, 2016. Available: http://go.fisita.com/store/papers/FISITA2016/F2016-ESYB-005.

[16] G. Shibata, Y. Shibike, H. Ushijima, and H. Ogawa, Identification of Factors Influencing Premixed Diesel Engine Noise and Mechanism of Noise Reduction by EGR and Supercharging, SAE Technical paper, 2013-01-0313, SAE International, USA, 2013. Available: https://doi.org/10.4271/2013-01-0313.

[17] J. Dernotte, J. Dec, and C. Ji, Efficiency Improvement of Boosted Low-Temperature Gasoline Combustion Engines (LTGC) Using a Double Direct-Injection Strategy, SAE Technical paper, 2017-01-0728, SAE International, USA, 2017. Available: https://doi.org/10.4271/2017-01-0728.

[18] J. E. Dec, J. Dernotte, and C. Ji, Increasing the Load Range, Load-to-Boost Ratio, and Efficiency of Low-Temperature Gasoline Combustion (LTGC) Engines, SAE International Journal of Engines, 2017-01-00731, SAE International, USA, 2017. Available: https://doi.org/10.4271/2017-01-0731.

[19] J. A. Eng, Characterization of Pressure Waves in HCCI Combustion, SAE Technical paper, 2002-01-2859, SAE International, USA, 2002. Available: https://doi.org/10.4271/2002-01-2859.

[20] N. Septivani and B. W. Riyandwita, “Spark ignition engine modeling for in-cylinder pressure and temperature prediction using Simulink,” MATEC Web of Conference, vol. 204, no. 04001, 2018. Available: https://doi.org/10.1051/matecconf/201820404001.

[21] R. K. Maurya, Reciprocating Engine Combustion Diagnostics, In-cylinder pressure measurement and analysis, Switzerland: Springer, pp. 294-295, 2019.

[22] J. E. Dec, Y. Yang, and N. Dronniou, “Improving efficiency and using E10 for higher loads in boosted HCCI engines,” SAE International Journal of Engines, vol. 5, no. 3, pp. 1009-1032, 2012. Available: https://doi.org/10.4271/2012-01-1107.